A Novel Cardiac Phantom to Study Murine and Human Cardiac Motion and Function using MRI

C. Constantinides[1], D. Nearchou[1], C. Constantinou[1], P. Ktorides[1], R. Gravett[2], and V. Tzagarakis[3]
[1]Mechanical and Manufacturing Engineering, University of Cyprus, Nicosia, Cyprus, [2]Shelley Medical Imaging Technologies, London, Ontario, Canada, [3]Alpha Evresis Diagnostic Center, Nicosia, Cyprus

Introduction: Despite a plethora of cardiac functional techniques for characterization of mechanical structure, function, and dysfunction, a parallel need exists for development of invasive and non-invasive tools and techniques to describe the left ventricular (LV) tissue material properties as these relate to the: 1) mechanical pumping function of the LV; 2) myocardial oxygen demand defining myocyte metabolic status; 3) coronary blood flow and its auto-regulation; 4) arhythmogenic risk; 5) cell-signaling pathways responsible for growth and remodeling during development and disease. This work studied human and murine myocardial motion and function in a novel cardiac phantom using MRI. Collectively, a technological platform was developed to allow detailed ex-vivo electro-mechanical studies of the cardiovascular system at the tissue and organ levels in mice and humans.

Theory: Continuum mechanical theory [1] leads to computation of torsional angles (φ), applied compressive-extensive pressures (P_{ce}), and developed torque (T) for deformable, elastic cylindrical rods, according to $\varphi=TL/GI_p$, $P_{ce}=E\varepsilon\pi r^2$, where G is the shear modulus, E is the Young modulus, ε is the deformation, and I_p is the moment of inertia of the material. Such equations provide operational upper limits and define design characteristics for the construction of a scaled-down murine cardiac model in combination with the use of commercially available elastomers, to mimic murine myocardial tissue, given prior published tagging and DENSE murine and human myocardial displacements, and LV end-systolic torsions (Table 1) [2-5].

Methods: Multi-modality Heart Phantom: A dynamic multimodality human heart phantom (Shelley Medical) that matches cardiac left and right ventricular anatomy was used for experimentation at the scale of the human heart. The phantom heart material (PVA) has stiffness that mimics the biomechanical properties of soft tissue and allows study of cardiac anatomy, its biomechanical properties, and cardiac motion. The phantom is equipped with computer controlled electronic (bench studies) and pneumatic (MRI studies) actuators that allow compression, stretching, and torsional deformation. Electrical activity (emulated with real life ECG signals) can synchronize acquisitions to the electrical heart cycle (electronic version) and a gating logic (+5V pulse) to trigger acquisition in MRI (pneumatic version). Pulsatile fluid flow is ensured through circulation of water through the two-chambered artificial heart throughout the cardiac cycle. The electronic version is equipped with programmable capability (VSA, Brookshire Software, USA), memory, and interface software for waveform downloading (RAPU, Brookshire Software, USA) that allows user defined motional waveforms with fine adjustment of cyclic speed (90-200bpm), cycle duration, and compression-extension displacements and torsions. The pneumatic system is controlled via a controller and an air-compressor and is equipped with controlling software (Pneumatics Heart Control, Shelley Medical) that allows adjustment of heart rates (10-100bpm) with a potential to be reprogrammed to allow higher (>400bpm) rates.

Autocad Design and Manufacturing of a Novel Scaled-Down Murine Cardiac Phantom: Additional parts were designed using Autocad (Autocad Desktop, USA), manufactured (Quickparts Inc, USA) and interfaced with the pneumatic controller system to allow use in a high field animal scanner and facilitate motion propagation within the magnet bore (Figure 1). Additional plexiglass supports were constructed that allowed accurate system placement in the bore of the magnet and fine adjustments in position of the mechanical rod that drove motion. The end-termination of the phantom rod was attached to either a rubber elastomer or to urethane rods of varying elasticity (PSI Urethanes, USA) using special glue. The entire assembly was fixed in a cylindrical plexiglass casing, in a commercial M2M birdcage coil.

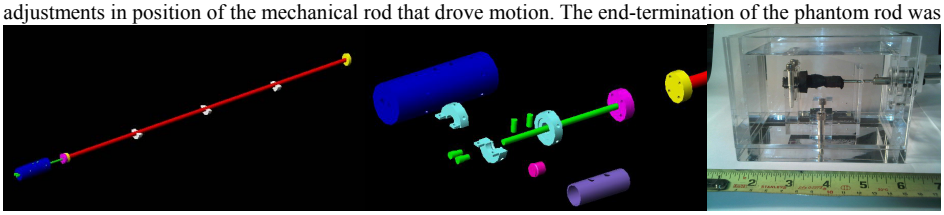

Cardiac Motional Indices	HUMANS	MICE
End-systolic torsion (°)	12.7±1.7	2.0±1.5
Ventricular length (mm)	60-70	7-8
Basal longitudinal displacement (mm)	-8.68±2.1	-0.5±0.12
Mid-ventricular longit. displ. (mm)	-6.23±1.95	-0.25±0.18
Apical longitudinal displ. (mm)	-3.88±1.55	0.06±0.25

Figure 1*: (Left to right) Autocad prototype design, prototype parts, and commercial scaled-down mouse model;* ***Table 1:*** *Human and mouse cardiac motional indices.*

Elastomer Characterization: Materials used were characterized using a Dynamic Mechanical Analysis (DMA) machine (Tritec 2000, Belgium) for the determination of their dynamic Young modulus variation with time and temperature. Briefly, rubber specimens (n=3) of the same type and material were placed and clamped at both ends by plastic-covered metal fixatives. Computer controlled software varied the temperature of a heating element placed underneath the sample, recording its temporal response (Figure 2) under controlled compression-stretching conditions.

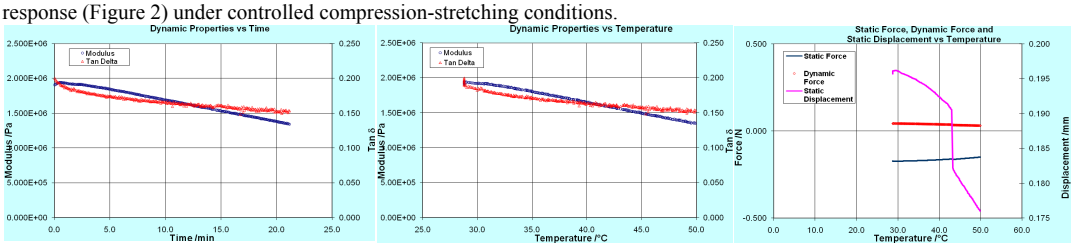

Figure 2*: Stress-strain mechanical characterization of a cylindrical rubber sample used to emulate murine myocardium in the constructed prototype system.*

Imaging of the Cardiac Phantom*:* The human phantom was imaged on a 1.5T scanner (Excelart Atlas, Toshiba) using an FFE-SSFP cardiac imaging sequence and a 32-loop phased array coil over 15 cardiac phases throughout the cardiac cycle. The elastomeric heart was contained in a plexiglass container filled with water. The imaging acquisition parameters were: TE=1.6 ms, TR=3.2ms, ST=8mm, FOV=35cm, NEX=1, 128x256 matrix, 10 contiguous slices. Fifteen phases of the heart cycle were acquired at temporal resolution of 53 ms and spatial resolution of 1.4x2.7x8 mm^3 with BW=±1302kHz, and a flip angle=70°. Cardiac gating was supplied to the peripheral gating module of the scanner from the ECG of a human volunteer (Heart Rate [HR]=73 bpm) and allowed timed-synchronous data acquisition with the phantom contraction-extension phases. **Image Processing***:* Quantification of Global Cardiac Function**:** LV blood cavity was segmented and binary masks generated using ImageJ (ImageJ, NIH, USA). Absolute volume were estimated by appropriate image voxel scaling given the water's density of ρ=1 g/cm^3. Myocardial stroke volume (SV), ejection fractions (EF), cardiac output (CO) were calculated according to: $SV = EDV - ESV$, $EF = SV / EDV$, and $CO = HR.SV$ where EDV and ESV represent the end-diastolic and end-systolic LV volumes, respectively.

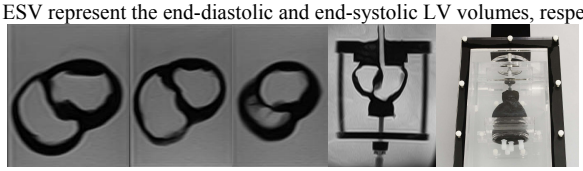

Cardiac Index	Human Phantom Heart
EF	11.3 %
EDV	75.1 ml
ESV	66.7 ml
SV	8.5 ml
CO	0.62 l/min

Figure 3*: (Left to right) Basal, mid, and apical short axis and long-axis MRI of the elastomeric heart (right), using a conventional FFE-SSFP cardiac imaging sequence on a 1.5T clinical system;* ***Table 2****: Global functional indices of the human cardiac phantom based on MRI.*

Results and Discussion: Figure 1 shows the design of the scaled down prototype mouse phantom and a prototype construction from Shelley Medical. Figure 2 depicts DMA characterization curves of the rubber sample used in the mouse phantom. Figure 3 shows imaging results (short, long axis) of the human heart phantom with functional indices tabulated in Table 2. Emulation of cardiac motion and function is possible computer-controlled human and mouse phantoms that will provide the platform for pulse sequence development, carefully controlled validation studies, and quantitative in vitro comparisons of myocardial function.

References: 1) Lai W., Rubin D. and Krempl E., *Introduction to Continuum Mechanics,* 3rd Ed., Pergamon Press, 1993, pp.254-264. **2)** Moore CC et al. Radiology 214:453-466, 2000. **3)** Henson et al. AJP 278(4):H1117-1123, 2000. **4)** Zhou R et al. MRM 49:760-764, 2003. **5)** Gilson WD et al. AJP 288(3):H1491-7, 2005.**Acknowledgements:** Funding was received from grants 'HEART', STOXOS0308/02, and PROSVASI0308/01 from the Research Promotion Foundation.